



ARTICLE

Open Access



Inhibitory effect of human indoleamine 2,3-dioxygenase 1 (hIDO1) by kazinol of 1,3-diphenylpropane derivatives

Taehoon Oh^{1,3†}, Sunin Jung^{2,4†}, Seon Min Oh^{2†}, Mi Hyeon Park², Hyoung-Geun Kim², Su-Yeon Lee², Sung-Kyun Ko^{1,5}  and Hyung Won Ryu^{2*} 

Abstract

This study focused on identifying and characterizing 1,3-diphenylpropane derivatives from flavonoids that inhibit human indoleamine 2,3-dioxygenase 1 (hIDO1) enzymes, which play a role in immune regulation and are associated with various diseases. A series of isolated metabolites (1–7) demonstrated modest to high inhibition of hIDO1, with binding degree values ranging from 26.31 to 72.17%. In particular, during a target-based screening of natural products using hIDO1, kazinol J (6, a 1,3-diphenylpropane derivative) was found to potently inhibit hIDO1, with a binding degree of 72.17% at 1 ppm. Kazinol J (6) showed concentration-dependent and mixed inhibition kinetics and achieved slow and time-dependent inhibition of hIDO1. Additionally, docking simulations were performed to evaluate the inhibitory potential and binding interactions of the compounds with hIDO1. These findings suggest that these 1,3-diphenylpropane derivatives can serve as therapeutic agents for conditions involving hIDO1 dysregulation, such as cancer, autoimmune disorders, and infectious diseases.

Keywords Kazinol, 1,3-diphenylpropane, Affinity-based ultrafiltration, Human indoleamine 2,3-dioxygenase 1, Docking simulations

Introduction

Human indoleamine 2,3-dioxygenase 1 (hIDO1) is an enzyme that has garnered significant interest in the fields of immunology and therapeutics because of its pivotal role in immune regulation and disease pathology [1–3]. hIDO1 acts as a key mediator in the modulation of immune responses, exerting immunosuppressive effects through its ability to catabolize tryptophan, an essential amino acid. By degrading tryptophan via the kynurenine pathway, hIDO1 inhibits T-cell proliferation, promotes regulatory T-cell differentiation, and induces immune tolerance [4, 5]. The dysregulation of pathways caused by hIDO1 in various pathological conditions may be related to this unique immunoregulatory function of hIDO1. The discovery of the immunosuppressive properties of hIDO1 has led to the development of hIDO1 inhibitors

[†]Taehoon Oh, Sunin Jung and Seon Min Oh have equally contributed as the first author.

*Correspondence:

Hyung Won Ryu
ryuhw@kribb.re.kr

¹Chemical Biology Research Center, Korea Research Institute of Bioscience and Biotechnology (KRIBB), Cheongju 28116, Korea

²Natural Medicine Research Center, Korea Research Institute of Bioscience and Biotechnology, Cheongju si, Chungcheongbuk-do 28116, Republic of Korea

³College of Pharmacy, Chungbuk National University, Cheongju, Chungbuk 28160, Korea

⁴Department of CBRN Medicine Research, Center for Special Military Medicine, Armed Forces Medical Research Institute, Daejeon 34059, South Korea

⁵KRIBB School of Bioscience, Korea University of Science and Technology (UST), Daejeon 34141, Korea

as potential therapeutic agents [6]. hIDO1 inhibitors are designed to selectively target and inhibit the enzymatic activity of hIDO1, thereby restoring immune responses and potentially offering novel treatments for a wide range of diseases. Promising results have been obtained with these inhibitors in preclinical studies, demonstrating their ability to reverse immunosuppression, enhance antitumor immunity, and modulate immune-mediated inflammatory diseases [7, 8]. Primarily, hIDO1 inhibitors have shown significant promise as cancer immunotherapies [9]. Tumors exploit the immunosuppressive effects of hIDO1 to evade immune surveillance and promote immune tolerance within the tumor microenvironment. By inhibiting hIDO1, the immune response against tumors may be reinvigorated, leading to enhanced antitumor immunity and improved treatment outcomes. As a result, clinical trials have been performed for several hIDO1 inhibitors, either as monotherapies or in combination with other immunotherapies, to improve the efficacy of cancer treatments and overcome resistance mechanisms [4, 10]. In addition to cancer treatment, hIDO1 inhibitors have shown potential in the treatment of autoimmune disorders and infectious diseases. In autoimmune diseases, such as rheumatoid arthritis and systemic lupus erythematosus, hIDO1 inhibitors hold promise for restoring immune balance and suppressing pathological immune responses [11, 12]. Similarly, hIDO1 inhibitors have the potential to enhance host immune responses against pathogens in infectious diseases, as immune evasion is a critical factor.

The discovery of bioactive natural products as leads for therapeutic development can be inspired by ethnopharmacology or achieved by screening plant extracts for bioactivity via *in vitro* and *in vivo* assays. There are several failures and pitfalls associated with the isolation of bioactive substances using activity-induced fractionation and scale-up. This is because the bioactive compounds are decomposed during separation through repetitive columns, or the bioactive compounds are present at very low concentrations, making it impossible to separate them efficiently. Recently, a method in which affinity-based ultrafiltration has been used to identify target metabolites from extracts has been developed [13–17].

Most inhibitors reported in the literature are natural products, and several compounds have been tested and demonstrated to be hIDO1 inhibitors [18–20]. Therefore, the inhibitory activities of most hIDO1 inhibitors have been reported in relation to the structural characteristics of natural plant inhibitors, such as differences between natural product-based carbonyl functional compounds and their inhibitory activities [21]. The reported review papers listed the effects of various substances isolated from natural products on the inhibitory activity of hIDO1, such as alkaloids (IC_{50} and K_i

= 2.0–32.0 μ M) [20], flavanones (IC_{50} =7.7–31.4 μ M) [21], quinones (IC_{50} =40.0 nM–24.6 μ M) [22], and herqueinone (IC_{50} =19.05–36.86 μ M) [23]. Therefore, we are confident that novel natural substances can lead to lead structures for the design and development of novel hIDO1 inhibitors. Additionally, among its many constituents, kazinol has been reported to exhibit more potent bioactivity and is of considerable interest to researchers for drug development because of its potential for therapeutic use. Kazinols, which have a 1,3-diphenylpropane backbone, have attracted interest because of their multifaceted chemical and biological activities. Kazinol derivatives have been widely reported to be effective at treating oxidative stress, inflammation, bacteria, fungi, viruses, and diabetes but have not been reported as natural substances that can act as hIDO1 target inhibitors. In this study, we utilized a rapid screening method and investigated an efficient approach to identify hIDO1 inhibitors from 1,3-diphenylpropane and chalcone using ultrafiltration procedures followed by UPLC–PDA and UPLC–ESI–QToF–MS. hIDO1 binding affinity examination by UPLC identified seven metabolites (1–7) that appeared to interact with hIDO1. These seven promising metabolites were isolated, and their binding inhibition and docking simulations were examined, all of which were significantly consistent with their significant inhibition.

Materials and methods

Chemicals

Broussonetia papyrifera (KRIBB 0059119) extract was obtained from the Natural Products Central Bank of the Korea Research Institute of Bioscience and Biotechnology (Daejeon, Korea) (<https://www.kobis.re.kr/npcb/uss/main.do>, accessed on 21 June 2024). The kazinols, 1,3-diphenylpropane, used in the experiments were extracted from the root bark of *Broussonetia papyrifera* as previously described [19, 20, Supplementary data]. 1,3-Diphenylpropane was purified using preparative high-performance liquid chromatography (HPLC) and achieved purities greater than 95%, as determined using an ultra-performance liquid chromatography–photodiode array (UPLC–PDA).

Broussonin B (1): yellowish powder; HRESIMS m/z 257.1168 (calcd for $C_{16}H_{18}O_3$, 257.1178); 1H NMR (400 MHz, acetone- d_6) and ^{13}C NMR (100 MHz, acetone- d_6) are shown in the Supplementary Table S1.

Broussonin A (2): yellowish powder; HRESIMS m/z 257.1167 (calcd for $C_{16}H_{18}O_3$, 257.1179); 1H NMR (400 MHz, acetone- d_6) and ^{13}C NMR (100 MHz, acetone- d_6) are shown in the Supplementary Table S1.

Broussochalcone A (3): yellow powder; HRESIMS m/z 339.1229 (calcd for $C_{20}H_{20}O_5$, 339.1232); 1H NMR (500 MHz, acetone- d_6) and ^{13}C NMR (125 MHz, acetone- d_6) are shown in the Supplementary Table S1.

Kazinol F (4): yellow powder; HRESIMS m/z 395.2247 $[M-H]^-$ (calcd for $C_{25}H_{32}O_4$, 395.2222); 1H NMR (500 MHz, acetone- d_6) and ^{13}C NMR (125 MHz, acetone- d_6) are shown in the Supplementary Table S1.

Kazinol V (5): yellow powder; HRESIMS m/z 425.2345 $[M-H]^-$ (calcd for $C_{26}H_{33}O_5$, 425.2328); 1H NMR (500 MHz, acetone- d_6) and ^{13}C NMR (125 MHz, acetone- d_6) are shown in the Supplementary Table S1.

Kazinol J (6): yellow powder; HRESIMS m/z 409.2410 $[M-H]^-$ (calcd for $C_{26}H_{33}O_4$, 409.2379); 1H NMR (500 MHz, acetone- d_6) and ^{13}C NMR (125 MHz, acetone- d_6) data are shown in the Supplementary Table S1.

Kazinol W (7): yellow powder; HRESIMS m/z 427.2473 $[M-H]^-$ (calcd for $C_{26}H_{35}O_5$, 427.2484); 1H NMR (500 MHz, acetone- d_6) and ^{13}C NMR (125 MHz, acetone- d_6) are shown in the Supplementary Table S1.

General apparatus

The 1D and 2D NMR spectra for compound identification were recorded on a Bruker AM500 instrument (Billerica, MA, USA). NMR solvents were purchased from Cambridge Isotope Lab. Inc. (Andover, MA, USA). The reagents needed for UPLC-PDA and UPLC-QToF-MS analysis were acetonitrile (Merck Millipore, Burlington, MA, USA), formic acid, and leucine enkephalin (Sigma-Aldrich, St. Louis, MO, USA). Distilled water was obtained using a Milli-Q Academic (Merck Millipore) water purification system. Tris(hydroxymethyl) aminomethane (Sigma-Aldrich, St. Louis, MO, USA), sodium chloride (99.5%, Junsei Chemical Co., Tokyo, Japan), imidazole (Sigma-Aldrich), potassium phosphate monobasic (Sigma-Aldrich), potassium phosphate dibasic (Sigma-Aldrich), L-ascorbic acid (Sigma-Aldrich), catalase from bovine liver (Sigma-Aldrich), methylene blue (Sigma-Aldrich), and L-tryptophan (Sigma-Aldrich) were used as the elution and enzyme assay buffers for His-hIDO1.

Purification of His-hIDO1

Human IDO1 (hIDO1) was obtained from the Korea Human Gene Bank (Medical Genomics Research Center, KRIBB, Korea). The hIDO1 sequence was subsequently cloned and inserted into the pET28a expression vector to generate the pET28a-hIDO1 plasmid, which was verified by DNA sequencing (performed by Cosmogentech, Seoul, Korea). The recombinant plasmid was transformed into *Escherichia coli* competent T7 strain (NEB, MA, USA) cells, and the protein expression of hIDO1 was induced by the addition of 1 mM isopropyl- β -D-1-thiogalactopyranoside (IPTG, Elpis, Daejeon, Korea) for 4 h at 37 °C. After induction, the expressed hIDO1 protein was purified using Ni-NTA agarose (Qiagen, Valencia, CA) at 4 °C. The eluted hIDO1 protein was subjected to dialysis against storage buffer (20 mM Tris-HCl buffer

(pH 8.0) and 200 mM NaCl). The purity of the hIDO1 protein was subsequently assessed by sodium dodecyl sulfate-polyacrylamide gel electrophoresis.

Ultrafiltration procedures

The samples were dissolved in dimethylsulfoxide (DMSO) to prepare sample solutions for ultrafiltration screening (Supplementary Table S2). In total, 400 μ L of the compound mixture was made by adding 50 μ L of His-hIDO1 (0.95, 1.9, and 3.8 mg/mL) in elution buffer (50 mM Tris-HCl, pH 8.8, 300 mM NaCl, and 300 mM imidazole) and 20 μ L of seven compounds (0.2 mg/mL) to 330 μ L of enzyme assay buffer (50 mM potassium phosphate buffer, pH 6.5, 20 mM ascorbic acid, 10 mM catalase, 10 μ M methylene blue, and 200 μ M L-tryptophan). The extract mixtures (at final concentrations of 4.0 mg/mL and His-hIDO1 at 0.2375 mg/mL) and the compound mixtures (at final concentrations of 0.01 mg/mL and His-hIDO1 at 0.475 mg/mL) were incubated for 10 min at 37 °C in a water bath. Then, the incubated mixtures were centrifuged at 13,000 rpm for 30 min, and the supernatant was filtered through a CHROMDISC[®] syringe filter (Hydrophilic PTFE 0.2 μ m; Echromscience, Daegu, Korea) for UPLC-PDA analysis. The control experiment was carried out similarly but without His-hIDO1. On the basis of the variations in peak areas before and after incubation with His-hIDO1, the reduced peak areas were determined as the degree of affinity between the ligand and the enzyme. The interaction can be defined by the binding degree (BD) and calculated as follows:

$BD\% = (Aa - Ab) / Aa * 100$ where Aa and Ab represent the peak areas of the samples (compounds 1–7) and interactions without and with active His-hIDO1, respectively.

UPLC-PDA and UPLC-ESI-QToF-MS analysis

The samples for ultrafiltration screening were analyzed by UPLC-PAD analysis, which was achieved with ultra-high-performance liquid chromatography coupled with a photodiode array detector (UPLC-PDA, ACQUITY UPLCTM System, Waters, Milford, MA, USA). Chromatographic separations were carried out with an ACQUITY I-Class UPLC System (Waters Co.). Water with 0.1% formic acid (A) and acetonitrile with 0.1% formic acid (B) were used as the mobile phases, which were eluted with the following gradient conditions: 0.0–1.0 min, 35% B; 1.0–12.0 min, 35–85% B; 12.0–12.1 min, 85–100% B; 12.1–13.4 min, 100% B; 13.4–13.5 min, 100–35% B; 13.5–15 min, 35% B; and a flow rate of 0.4 mL/min for 15 min. Each of the seven compounds (0.1 mg/mL) was analyzed using a Vion IMS QTOF mass spectrometer (Waters Co.). The analysis was performed using the same mobile phase and chromatographic gradient conditions as the UPLC-PAD mentioned above. Mass

spectrometry (in anion mode) was performed by electrospray ionization (ESI).

The type of desolvation gas used was nitrogen gas. The MS parameters used were as follows: 2.3 kV capillary, 40 V cone voltage, 110 °C source temperature, 350 °C, desolvation temperature, 50 L/h cone gas flow, and 800 L/h desolvation gas flow. To calibrate the accuracy and reproducibility of the data, leucine-enkephalin (m/z 554.2615 (ESI-)) was used as an internal standard solution, and the scan range of mass values was set to m/z 100–1500. The collision gas energy for MS/MS was 10–45 V. The data were collected for each sample with a 0.25 s scan time and a 0.01 s interscan delay. All MS data were analyzed in MS^E mode, and the data were collected using UNIFI software (v1.9, Waters Co.).

His-tagged hIDO1 enzyme assay

The enzyme activity assays were conducted according to a protocol outlined by Kwon et al. [21]. In brief, the 200 μ L reaction mixture comprised potassium phosphate buffer (50 mM, pH 6.5), ascorbic acid (20 mM), methylene blue (10 μ M), catalase (10 mM), purified recombinant hIDO1 enzyme (5 μ g/mL) and L-tryptophan (Trp, 200 μ M). The metabolites were serially diluted in dimethyl sulfoxide (DMSO, 0.1%, v/v) and dispensed into 96-well plates. The reaction was carried out at 37 °C for 1 h, halted with 40 μ L of trichloroacetic acid (30%) and heated at 65 °C for 15 min. Centrifugation at 4000 rpm for 15 min was performed to eliminate the debris. Subsequently, 125 μ L of the supernatant from each well was transferred to another 96-well plate. *p*-Dimethylaminobenzaldehyde (125 μ L; 2%, v/v) in acetic acid was then added to each well, and the absorbance at 480 nm was measured using a SpectraMAX-190 ELISA reader (Molecular Devices, Sunnyvale, CA). Each assay was performed in triplicate. The inhibitory concentration at which 50% loss of activity (IC₅₀) occurred was determined by fitting the experimental data to a logistic curve as described in previous studies [13]. The inhibition constants for the binding of inhibitors to free enzymes or enzyme–substrate complexes, denoted as K_I or K_{IS} , respectively, were obtained from secondary plots created from the slopes of straight lines or vertical intercepts ($1/V_{max}^{app}$) versus the inhibitor concentration according to Eqs. (2), (3) and (4) [13, 24–26].

$$\text{Activity (\%)} = 100 [1 / (1 + ([I] / IC_{50}))] \quad (1)$$

$$1/V = K_m/V_{max} (1 + [I]/K_I) 1/S + 1/V_{max} \quad (2)$$

$$\text{Slope} = K_m/K_I V_{max} [I] + K_m/V_{max} \quad (3)$$

$$\text{Intercept} = 1/K_{IS} V_{max} [I] + 1/V_{max} \quad (4)$$

Time-dependent assay for affinity-based inhibition

Time-dependent assays were conducted using 129 μ Units of recombinant hIDO1 enzyme and 50 mM potassium phosphate buffer (pH 6.5) at 37 °C. To investigate the affinity-based time-dependent inhibition of hIDO1, progression curves were generated from the chromatograms after preincubation for 5, 10, and 15 min with constant inhibitor concentrations of 5 and 10 (20 μ M).

Docking simulations utilizing hIDO1

The crystal structure of hIDO1, obtained from the Protein Data Bank under the accession code 5WN8, served as the foundation for docking simulations [27]. Noncovalent docking was performed using AutoDock Vina. Proteins and ligand pdbqt files were prepared using standard AutoDock tools. The starting coordinates of hIDO1 were docked into the prepared receptor grid by AutoDock Vina. Discovery Studio Visualizer v17.2 and LigPlot v2.2.8 were used for analyzing protein–ligand interactions and obtaining charges.

Results and discussion

UPLC–ESI–QToF–MS analysis of 1,3-diphenylpropanes and chalcones

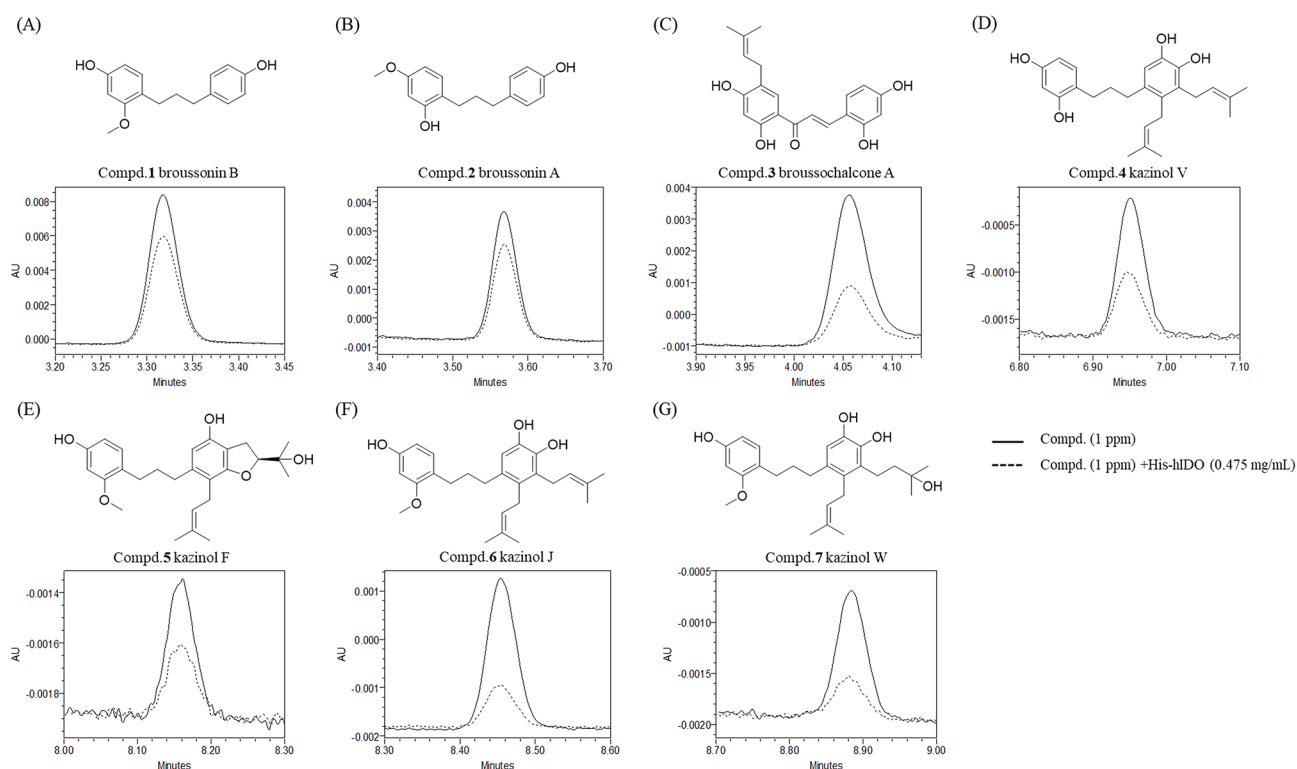
UPLC–PDA–QToF–MS can be used to quickly identify potential bioactive substances [28–32]. The structures and identities of six 1,3-diphenylpropanes (1, 2, and 4–7) and a chalcone (3) were confirmed via spectroscopic analyses in negative modes, such as MS, MS/MS, UV spectroscopy, and high-resolution mass spectrometry (HRMS). The spectroscopic data of these compounds were compared with those in the previous literature [33, 34]. As shown in Table 1, Compounds 1 and 2 were detected at m/z 515 [2 M–H][–], 257 [M–H][–], 135 [^{2,3}A][–], and 119 [^{2,3}B][–] (calcd for C₁₆H₁₈O₃, 257.1178), and compound 3 was detected at m/z 339 [M–H][–], 203 [^{1,2}A][–], 159 [^{1,2}A–CO₂][–] and 135 [^{1,2}B][–] (calcd for C₂₀H₂₀O₅, 339.1232). Compound 4 was detected at m/z 395 [M–H][–] and 203 [^{2,3}B–prenyl+H][–] (calcd for C₂₅H₃₂O₄, 395.2222), and compound 5 was detected at m/z 425 [M–H][–], 407 [M–H₂O–H][–], 269 [^{1,3}B–H₂O][–], and 149 [^{3,4}A][–] (calcd for C₂₆H₃₄O₄, 409.2379). Compound 6 was detected at m/z 409 [M–H][–], 271 [^{2,3}B][–], and 149 [^{3,4}A][–] (calcd for C₂₆H₃₄O₄, 409.2379), and compound 7 was detected at m/z 427 [M–H][–], 409 [M–H₂O–H][–], and 149 [^{3,4}B][–] (calcd for C₂₆H₃₆O₅, 427.2484). Comparison with the literature led to the identification of broussonin B (1), broussonin A (2), brousochalcone A (3), kazinol F (4), kazinol V (5), kazinol J (6), and kazinol W (7) (Supplementary Figure S1).

hIDO1 binding of 1,3-diphenylpropanes and chalcones

Ultrafiltration screening coupled with UPLC is a rapid method used to screen bioactive materials in complex

Table 1 UPLC chromatography, UV-vis, mass spectral data, and degree of binding of hIDO1 target inhibitory effects on 1,3-diphenylpropane and chalcone (1–7)

NO.	Compounds	Rt (min)	UV (nm)	Detected ion [M-H] ⁻	Calculated ion [M-H] ⁻	MS/MS	Error (ppm)	Peak area (Intensity)		BD (%)
								control	hIDO1 (0.475 mg/mL)	
1	Broussonin B	3.32	236, 276	257.1168	257.1178	119, 135	-3.9	19,053	14,040	26.31%
2	Broussonin A	3.57	233, 279	257.1167	257.1178	119, 135	-4.3	9912	7229	27.06%
3	Brousochalcone A	4.05	263	339.1229	339.1232	135, 203	-0.9	12,025	4380	63.57%
4	Kazinol F	6.95	225, 282	395.2247	395.2222	121, 203, 273	6.3	3641	1759	51.68%
5	Kazinol V	8.14	233, 282	425.2345	425.2328	149, 269, 407	4.0	1447	749	48.23%
6	Kazinol J	8.45	225, 281	409.2425	409.2379	149, 271	1.5	8503	2366	72.17%
7	Kazinol W	8.88	282	427.2478	427.2484	409, 353, 271, 203, 149	-2.6	3417	1220	64.29%

**Fig. 1** UV 280 nm chromatograms of the seven compounds (1–7) without (solid line) and with (dotted line) hIDO1 in buffer. Peaks numbered 1–7 represent the compounds isolated from *Broussonetia papyrifera* roots in our study

mixtures and is performed with a trace amount of analysis sample [14–17]. The enzyme and ligand–enzyme complex, which are generated by interactions between the enzyme and potential enzyme inhibitors in complex mixtures, can be separated by ultrafiltration. In this study, potential hIDO1 inhibitors were quickly identified via ultrafiltration screening via UPLC-PDA-QToF-MS. Solutions containing seven compounds that interact without and with active hIDO1 were analyzed and compared (Fig. 1). The solution was determined to be the optimal condition, as broussonin A (2) was isolated in large amounts. The experiment was carried out by lowering the total concentration of broussonin A (2) from 1 ppm to 100 ppm, and hIDO1 was fixed at 0.119

and 0.475 mg/mL (Supplementary Figure S2-4). When the total concentration of the compound was 1 ppm, a decrease in the peak area was clearly observed with the naked eye, and the binding degree (BD) caused by the enzyme–compound interaction was greater than 20% (Supplementary Figure S4). Finally, the total concentration of the compound solution was 1 ppm, and hIDO1 was used at 0.477 mg/mL. The seven compound solutions were detected at 280 nm and checked to reduce the peak area in the compound solution with hIDO1. The BD can be measured by substituting this information into the BD formula. As shown in Table 1, the BDs of seven compounds (1–7) exceeded 25%, and the BD of brousochalcone A (3), a prenylated chalcone, was

63.57%. The two compounds (broussonin B (1) and A (2)) and 1,3-diphenylpropanes generated BDs of 26.31% and 27.06%, respectively. On the other hand, the BDs of four prenylated 1,3-diphenylpropanes [kazinol F (4), kazinol V (5), kazinol J (6), and kazinol W (7)] were 51.68%, 48.23%, 72.17%, and 64.29%, respectively. As a result, it can be tentatively concluded that the prenyl group and chalcone affect the interaction with the enzyme.

hIDO1 inhibitory activities

The potential therapeutic effects of 1,3-diphenylpropanes from flavonoid classes have been suggested for cancer treatments and as anti-inflammatory agents. However, the hIDO1 inhibitory activity of 1,3-diphenylpropanes has not been determined. For this reason, the hIDO1 inhibitory activity of kazinol J (6), the most potent of the isolated 1,3-diphenylpropanes, was tested (Fig. 2A; Table 1). Our findings revealed intriguing insights into the structure–activity relationship. Specifically, the presence of a prenyl group on the stilbene may be crucial for

the inhibition of hIDO1, as evidenced by the IC_{50} value of kazinol J (6, $IC_{50}=43.0 \mu\text{M}$). We also tested epacadostat (Epa) as a positive control and broussonin A (1) and B (2), which are nonprenyl 1,3-diphenylpropanes backbones, as negative controls.

Enzyme kinetic analysis

As shown in Fig. 2B, the inhibition kinetics mechanism revealed by the Lineweaver–Burk plots indicates that kazinol J (6) is a typical mixed-type inhibitor; increasing the concentration of kazinol J (6) resulted in a family of lines with a common intercept on the y -axis but with different gradients. Therefore, through additional diagrams and equations, we evaluated and confirmed which hypothesis in the previously known enzyme mechanism can provide this kinetic profile. A typical mixed inhibition mechanism modifies the substrate with an inhibitor, and the parameters K_I and K_{IS} can be investigated by measuring the residual enzyme–substrate complex via Eqs. (3) and (4) [13, 24]. The equilibrium constants for

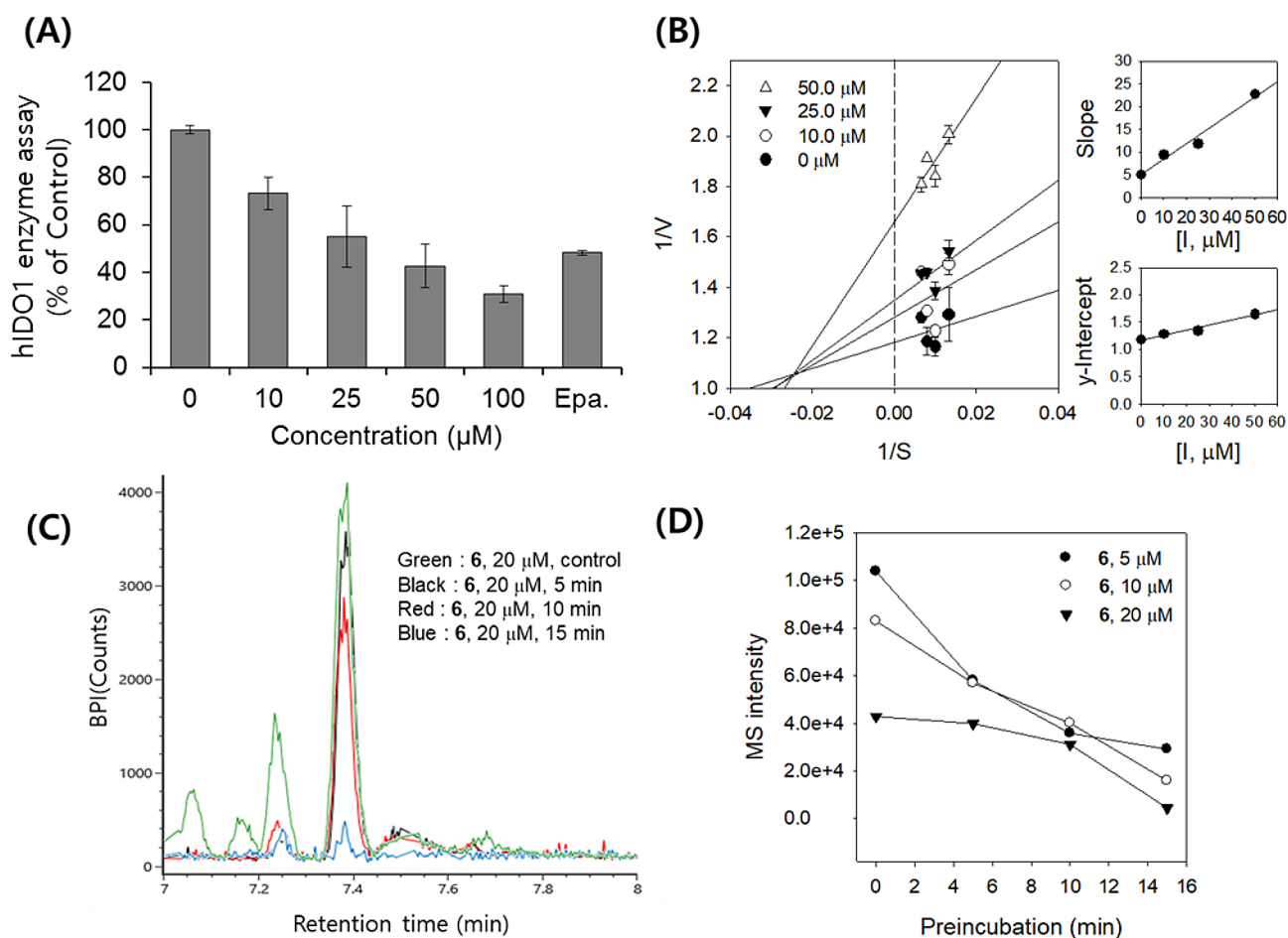


Fig. 2 (A) Concentration-dependent hIDO1 activity of kazinol J (6). (B) Lineweaver–Burk plots showing the ability of kazinol J (6) to inhibit hIDO1. (C) Time-dependent chromatograms of hIDO1 in the presence of kazinol J (6) using UPLC–QToF–MS. (D) Inhibition as a function of preincubation time for the most active kazinol J (6) (5, 10, and 20 μM)

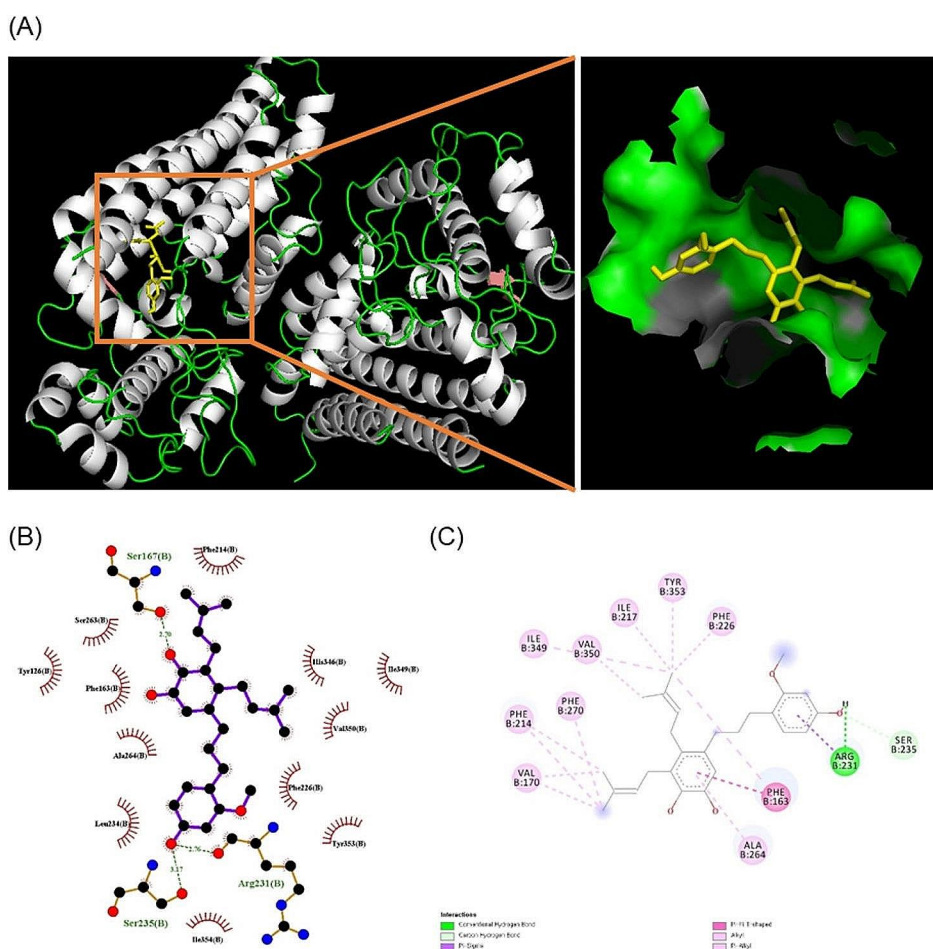


Fig. 3 Molecular docking views of the target compound kazinol J (6) on hIDO1. **(A)** Input structures of kazinol J (6) in hIDO1. **(B)** 2D representation of the Ligplot analysis results. **(C)** 2D representation of the Studio discovery results

its binding with free enzyme (K_I) and with the enzyme-substrate complex (K_{IS}) were obtained from the second plots of K_m/V_{max} and $1/V_{max}$ versus the concentration of kazinol J (6). Lineweaver–Burk plots of the initial velocity versus hIDO1 enzyme concentrations at different concentrations of kazinol J (6) generated a series of straight lines, all of which intersect the second quadrant (Fig. 2B). The mechanisms were analyzed through Dixon plots and secondary diagrams to determine the binding affinity of the EI and ESI complexes in enzyme reactions [35, 36]. A Dixon plot (Fig. 2B, Slope) of the Lineweaver–Burk relationship versus the slope of the line of the inhibitor concentration shows that it has an EI dissociation constant (K_I) of 13.7 μM , whereas the secondary diagram (Fig. 2B, y-Intercept) of the intercept versus the inhibitor concentration generated an ESI dissociation constant (K_{IS}) of 127.3 μM . One putative binding mode of kazinol J (6) may involve binding between the inhibitor and the active site of free hIDO1 or the hIDO1-substrate complex. On the basis of the approximately 9.3-fold higher K_{IS} values, binding between kazinol J (6) and the hIDO1 substrate

intermediate may be weaker, and the inhibition mechanism is competitive and predominates over noncompetitive mechanisms.

Slow and time-dependent inhibitory activity

In the mechanism of known competitive inhibitors, the inhibitors slowly bind to the target enzyme active site. As shown in the data in Fig. 2C, inhibition by isolated kazinol J (6) was greater after preincubation for 5–15 min than without preincubation. As the residual activity decreased as a function of preincubation time, kazinol J (6) was identified as a slow-binding inhibitor. Increasing the concentration of kazinol J (6) led to decreases in the initial velocity and the steady-state rate (Fig. 2D). The preincubation step and time were equally important, as shown in Fig. 2D, indicating that the affinity of the inhibitor for the free enzyme was greater than that of the inhibitor for the enzyme-substrate complex. Hence, isolated kazinol J (6) acted as a time-dependent and slow inhibitor of the target enzyme, similar to other compounds reported in a previous study [13, 37].

Computational docking simulations for ligand candidates of hIDO1

To visualize the binding interactions of broussonin B (1), kazinol V (4), kazinol F (5), kazinol J (6), and kazinol W (7) with the hIDO1 enzymes, molecular docking analysis was performed. Molecular docking analysis via the AutoDock Vina program revealed that 1,3-diphenylpropanes (1, 4, 5, 6 and 7) bind to the allosteric site of hIDO1 (Fig. 3 and Supplementary Fig. S3). Broussonin B (1), which lacks a prenyl group in its backbone, was observed to bind to other sites (Supplementary Fig. S3C). In contrast, kazinol F (5) showed a different binding pattern from those of kazinol V (4), kazinol J (6), and kazinol W (7) because of the presence of a prenyl group at the meta position of the aromatic ring, which cyclizes to form 2,3-dihydrobenzofuran (Supplementary Fig. S3D). Furthermore, compared with that in kazinol J (6), the methylation of the ortho position in kazinol V (4) resulted in structural changes that disrupted hydrogen bonding. Specifically, the hydroxyl group attached to kazinol V interfered with hydrogen bonding, resulting in decreased affinity (Supplementary Fig. S3E). Kazinol J (6) and kazinol W (7) possess different structures because the prenyl group of kazinol W (7) changes to a hydroxyl group. The affinity of kazinol W (7) decreased due to interference with binding (Supplementary Fig. S3F). Therefore, in terms of docking structure, kazinol J (6) achieved the best effect. Therefore, the results show that 1,3-diphenylpropane derivatives constitute a new class of hIDO1 inhibitors.

The aim of this study was to identify and characterize 1,3-diphenylpropane derivatives from the flavonoid class as novel inhibitors of the enzyme hIDO1. hIDO1 is an enzyme involved in immune regulation and is implicated in various diseases. Inhibiting hIDO1 can potentially restore immune responses and offer novel therapeutic approaches. General apparatus and chemicals: This section lists the instruments and chemicals used in the study, including NMR spectrometry, UPLC-PDA, and UPLC-ESI-QToF-MS. His-hIDO1: His-hIDO1, the hIDO1 protein, was purified from *Escherichia coli* cells transformed with the hIDO1 gene. The purification involved the use of Ni-NTA agarose and dialysis. Isolation of 1,3-diphenylpropanes and chalcones: Seven compounds (1–7) were obtained, and their structures were determined through MS spectroscopic analysis. Ultrafiltration procedures: Sample solutions containing the compounds were prepared and incubated with hIDO1. The mixtures were then centrifuged, and the supernatants were analyzed via UPLC-PDA-QToF-MS. The interactions between the compounds and hIDO1 were evaluated on the basis of changes in peak areas. His-hIDO1 enzyme assays were performed using purified recombinant hIDO1 enzyme and L -Trp as the substrate. The reaction mixture

was incubated and stopped, and the metabolites were analyzed using *p*-dimethylaminobenzaldehyde. Docking simulation of hIDO1: Docking simulations using AutoDock Vina were performed to predict the binding interactions between the compounds and hIDO1 using the crystal structure of hIDO1 (PDB code 5WN8).

This study aimed to identify 1,3-diphenylpropane derivatives as novel hIDO1 inhibitors. The compounds were isolated, and their interactions with hIDO1 were assessed via various techniques. The results of this study provide insights into the potential of these 1,3-diphenylpropanes derivatives as therapeutic agents for diseases involving hIDO1 dysregulation, such as cancer, autoimmune disorders, and infectious diseases.

Abbreviations

hIDO1	Human indoleamine 2,3-dioxygenase 1
IC ₅₀	Half maximal inhibitory concentration
HPLC	High-performance liquid chromatography
UPLC-PDA	Ultraperformance liquid chromatography-photodiode array
HRESIMS	High-resolution electrospray ionization mass spectrometry
NMR	Nuclear magnetic resonance
IPTG	Isopropyl- β -D-1-thiogalactopyranoside
DMSO	Dimethylsulfoxide
BD	Degree of binding

Supplementary Information

The online version contains supplementary material available at <https://doi.org/10.1186/s13765-024-00923-5>.

Supplementary Material 1

Acknowledgements

This study was supported by grants from the Korea Research Institute of Bioscience and Biotechnology Research Initiative Program (KGM5292322 and KGM1222312) and the National Research Foundation of Korea (NRF-2017R1C1B2002602), the Young Researcher Program (NRF-2020R1C1C1013934), and the National Research Council of Science & Technology (NST) (CAP23011-300) of the NRF. We thank the Korea Basic Science Institute, Cheongju, Republic of Korea, for providing the NMR data.

Author contributions

Oh TH, J SI, Oh SM, Park MH, Kim HG, and Lee SY performed the compounds of the analysis samples; Oh TH, J SI, and Ko SK performed the biological analysis and helped with the preparation of the manuscript; Oh SM, Ko SK, and Ryu HW collected and discussed the results; Ko SK and Ryu HW designed and supervised all the results and wrote the manuscript. All authors read and approved the final manuscript.

Funding

This work was supported by the KRIBB Research Initiative Program funded by the Ministry of Science and ICT (MSIT) of Republic of Korea.

Data availability

The datasets used and/or analyzed during the current study are available from the corresponding author on reasonable request.

Declarations

Competing interests

The authors declare no competing interests. Hyung Won Ryu is an Associate Editor of *Applied Biological Chemistry*.

Received: 1 May 2024 / Accepted: 28 July 2024

Published online: 04 September 2024

References

- Munn DH, Mellor AL (2016) IDO in the Tumor Microenvironment: Inflammation, Counter-regulation, and Tolerance. *Trends Immunol* 37:193–207
- Prendergast GC, Mondal A, Dey S, Laury-Kleintop LD, Muller AJ (2018) Inflammatory reprogramming with IDO1 inhibitors: turning immunologically unresponsive 'Cold' tumors 'Hot'. *Trends Cancer* 4:38–58
- Wainwright DA, Balyasnikova IV, Chang AL, Ahmed AU, Moon KS, Auffinger B, Tobias AL, Han Y, Lesniak MS (2012) IDO expression in brain tumors increases the recruitment of regulatory T cells and negatively impacts survival. *Clin Cancer Res* 18:6110–6121
- Fujiwara Y, Kato S, Nesline MK, Conroy JM, DePietro P, Pabla S, Kurzrock R (2022) Indoleamine 2,3-dioxygenase (IDO) inhibitors and cancer immunotherapy. *Cancer Treat Rev* 110:102461
- Stone TW, Williams RO (2023) Modulation of T cells by tryptophan metabolites in the kynurenine pathway. *Trends Pharmacol Sci* 44:442–456
- Campeato LF, Budhu S, Tchaicha J, Weng CH, Gigoux M, Cohen IJ, Redmond D, Mangarin L, Pource S, Liu C, Zappasodi R, Zamarin D, Cavanaugh J, Castro AC, Manfredi MG, McGovern K, Merghoub T, Wolchok JD (2020) Blockade of the AHR restricts a Treg-macrophage suppressive axis induced by L-Kynurenine. *Nat Commun* 11:4011
- Masaki A, Ishida T, Maeda Y, Suzuki S, Ito A, Takino H, Ogura H, Totani H, Yoshida T, Kinoshita S, Narita T, Ri M, Kusumoto S, Inagaki A, Komatsu H, Niimi A, Ueda R, Utsunomiya A, Inagaki H, Iida S (2015) Prognostic significance of Tryptophan Catabolism in Adult T-cell Leukemia/Lymphoma. *Clin Cancer Res* 21:2830–2839
- Ricciuti B, Leonardi GC, Puccetti P, Fallarino F, Bianconi V, Sahebkar A, Baglivo S, Chiari R, Pirro M (2019) Targeting indoleamine-2,3-dioxygenase in cancer: scientific rationale and clinical evidence. *Pharmacol Ther* 196:105–116
- Yeung AW, Terentis AC, King NJ, Thomas SR (2015) Role of indoleamine 2,3-dioxygenase in health and disease. *Clin Sci* 129:601–672
- Kjeldsen JW, Lorentzen CL, Martinenaite E, Ellebaek E, Donia M, Holmstrom RB, Klausen TW, Madsen CO, Ahmed SM, Weis-Banke SE, Holmstrom MO, Hendel HW, Ehrnrooth E, Zocca MB, Pedersen AW, Andersen MH, Svane IM (2022) A phase 1/2 trial of an immune-modulatory vaccine against IDO/PD-L1 in combination with nivolumab in metastatic melanoma. *Nat Med* 27:2212–2223
- Yan Y, Zhang GX, Gran B, Fallarino F, Yu S, Li H, Cullimore ML, Rostami A, Xu H (2010) IDO upregulates regulatory T cells via tryptophan catabolite and suppresses encephalitogenic T-cell responses in experimental autoimmune encephalomyelitis. *J Immunol* 185:5953–5961
- Szanto S, Koreny T, Mikecz K, Glant TT, Szekanecz Z, Varga J (2007) Inhibition of indoleamine 2,3-dioxygenase-mediated tryptophan catabolism accelerates collagen-induced arthritis in mice. *Arthritis Res Ther* 9:R50
- Park MH, Jung SJ, Yuk HJ, Jang HJ, Kim WJ, Kim DY, Lim GT, Lee JH, Oh SR, Lee SU, Ryu HW (2021) Rapid identification of isoprenylated flavonoids constituents with inhibitory activity on bacterial neuraminidase from root barks of paper mulberry (*Broussonetia papyrifera*). *Int J Biol Macromol* 174:61–68
- He YJ, Cheng P, Wang W, Yan S, Tang Q, Liu DB, Xie HQ (2018) Rapid investigation and screening of bioactive components in simo decoction via LC-Q-TOF-MS and UF-HPLC-MD methods. *Molecules* 23:1792
- Ning ZW, Zhai LX, Huang T, Peng J, Hu D, Xiao HT, Wen B, Lin CY, Zhao L, Bian ZX (2019) Identification of α -glucosidase inhibitors from *Cyclocarya paliurus* tea leaves using UF-UPLC-Q/TOF-MS/MS and molecular docking. *Food Funct* 10:1893
- Yin XS, Zhang XQ, Yin JT, Kong DZ, Li DQ (2019) Screening and identification of potential tyrosinase inhibitors from *Semen Oroxylis* extract by ultrafiltration LC-MS and in silico molecular docking. *J Chromatogr Sci* 57:838–846
- Wang ZQ, Hwang SH, Huang B, Lim SS (2015) Identification of tyrosinase specific inhibitors from *Xanthium strumarium* fruit extract using ultrafiltration-high-performance liquid chromatography. *J Chromatogr B Analyt Technol Biomed Life Sci* 1002:319–328
- Jang JP, Jang JH, Soung NK, Kim HM, Jeong SJ, Asami Y, Shin KS, Kim MR, Oh H, Kim BY, Ahn JS (2012) Benzomalvin E, an indoleamine 2,3-dioxygenase inhibitor isolated from *Penicillium* sp. FN070315. *J Antibiot* 65:215–217
- Williams DE, Steino A, de Voogd NJ, Mauk AG, Andersen RJ (2012) Haliclic acids A and B isolated from the marine sponge *Haliclona* sp. collected in the Philippines inhibit indoleamine 2,3-dioxygenase. *J Nat Prod* 75:1451–1458
- Tan Y, Liu M, Li M, Chen Y, Ren M (2022) Indoleamine 2,3-dioxygenase 1 inhibitory compounds from natural sources. *Front Pharmacol* 13:1046818
- Kwon M, Ko SK, Jang M, Kim GH, Ryoo IJ, Son S, Ryu HW, Oh SR, Lee WK, Kim BY, Jang JH, Ahn JS (2019) Inhibitory effects of flavonoids isolated from *Sophora flavescens* on indoleamine 2,3-dioxygenase 1 activity. *J Enzyme Inhib Med Chem* 34:1481–1488
- Pereira A, Vottero E, Roberge M, Mauk AG, Andersen RJ (2006) Indoleamine 2,3-dioxygenase inhibitors from the northeastern pacific marine hydroid *Garveia annulata*. *J Nat Prod* 69:1496–1499
- Yu JS, Jeong SY, Li CS, Oh TH, Kwon MC, Ahn JS, Ko SK, Ko YJ, Cao SE, Kim HH (2022) New phenalenone derivatives from the hawaiian volcanic soil-associated fungus *penicillium herquei* FT729 and their inhibitory effects on indoleamine 2,3-dioxygenase 1 (IDO1). *Arch Pharm Res* 45:105–113
- Zhang JP, Chen QX, Song KK, Xie JJ (2006) Inhibitory effects of salicylic acid family compounds on the diphenolase activity of mushroom tyrosinase. *Food Chem* 95:579–584
- Krishna A, Lee JS, Kumar S, Sudevan ST, Uniyal P, Pappachen LK, Kim H, Mathew B (2023) Inhibition of monoamine oxidases by benzimidazole chalcone derivatives. *Appl Biol Chem* 66:37
- Peedikayil AT, Lee JS, Abdelgawad MA, Ghoneim MM, Shaker ME, Selim S, Kumar S, Dev S, Kim H, Mathew B (2023) Inhibitions of monoamine oxidases by ferulic acid hydrazide derivatives: synthesis, biochemistry, and computational evaluation. *Appl Biol Chem* 66:66
- Lewis-Ballester A, Pham KN, Batabyal D, Karkashon S, Bonanno JB, Poulos TL, Yeh SR (2017) Structural insights into substrate and inhibitor binding sites in human indoleamine 2,3-dioxygenase 1. *Nat Commun* 8:1693
- Pang SQ, Wang GQ, Lin J, Diao Y, Xu R (2014) Cytotoxic activity of the alkaloids from *Broussonetia papyrifera* fruits. *Pharm Biol* 52:1315–1319
- Mei QR, Wang YH, Du GH, Liu GM, Zhang L, Cheng YX (2009) Antioxidant lignans from the fruits of *Broussonetia papyrifera*. *J Nat Prod* 72:621–625
- Ko HH, Chang WL, Lu TM (2008) Antityrosinase and antioxidant effects of ent-kaurane diterpenes from leaves of *Broussonetia papyrifera*. *J Nat Prod* 71:1930–1933
- Lee DH, Bhat KPL, Fong HHS, Farnsworth NR, Pezzuto JM, Kinghorn AD (2001) Aromatase inhibitors from *Broussonetia papyrifera*. *J Nat Prod* 64:1286–1293
- Zhong HT, Lia F, Chena B, Wang MK (2011) Euphane triterpenes from the bark of *Broussonetia papyrifera*. *Helv Chim Acta* 94:2061–2065
- Ryu HW, Park MH, Kwon OK, Kim DY, Hwang JY, Jo YH, Ahn KS, Hwang BY, Oh SR (2019) Anti-inflammatory flavonoids from root bark of *Broussonetia papyrifera* in LPS-stimulated RAW264.7 cells. *Bioorg Chem* 92:103233
- Shan LL, Wu YY, Yuan L, Zhang Y, Xu YY, Li Y (2017) Rapid screening of chemical constituents in *Rhizoma Anemarrhenae* by UPLC-Q-TOF/MS combined with data postprocessing techniques. *Evid Based Complement Alternat Med* 2017:4032820
- Bowden AC (1974) A simple graphical method for determining the inhibition constants of mixed, uncompetitive and noncompetitive inhibitors. *Biochem J* 137:143–144
- Djouonzo PT, Mukim MSI, Kemda PN, Kowa TK, Tchinda AT, Agbor GA, Pan CH, Song DG (2023) SARS-CoV-2 main protease inhibitors from the stem barks of *Discoglyprema caloneura* (Pax) Prain (Euphorbiaceae) and *Pterocarpus erinaceus* Poir (Fabaceae) and their molecular docking investigation. *Appl Biol Chem* 66:76
- Park JY, Yuk HJ, Ryu HW, Lim SH, Kim KS, Park KH, Ryu YB, Lee WS (2017) Evaluation of polyphenols from *Broussonetia papyrifera* as coronavirus protease inhibitors. *J Enzyme Inhib Med Chem* 32:504–512

Publisher's Note

Springer Nature remains neutral with regard to jurisdictional claims in published maps and institutional affiliations.